Origin of P_{b1} center at SiO_2/Si(100) interface: First-principles calculations

Koichi Kato
Advanced LSI Technology Laboratory, Toshiba Corporate Research and Development Center, 1 Komukai Toshiba-cho, Saiwai-ku, Kawasaki 210-8582, Japan

Takahiro Yamasaki
Fujitsu Laboratories Ltd., 10-1 Morinosato-Wakamiya, Atsugi 243-0197, Japan

Tsuyoshi Uda
AdvanceSoft Corp. Center for Collaborative Research, University of Tokyo, 4-6-1 Komaba, Meguro-ku, Tokyo 153-8904, Japan
(Received 14 October 2005; published 3 February 2006)

Based on first-principles calculations, we studied the generation behavior of P_b centers at SiO_2/Si interfaces, especially for P_{b1} centers, under oxidation of Si(100) surfaces. P_{b1} centers were found to be formed through successive O bridge-bond formation in oxidation processes. P_{b1} centers are generated first after P_{b0} center generation, but both types of P_b center can exist simultaneously at the same SiO_2/Si interface. The atomic and electronic structures of P_{b1} centers agree with both the theoretically and the experimentally approved hyperfine structures, and the energy levels of gap states at P_b centers correspond well with the experimental observations.

DOI: 10.1103/PhysRevB.73.073302 PACS number(s): 68.35.−p, 68.55.−a, 73.20.−r, 73.22.−f

With the advent of Si LSI technology, control of the SiO_2/Si(100) interface at the atomic level has become a key issue in the formation of further integrated metal-oxide-semiconductor (MOS) devices.[1,2] The electrical device characteristics have, however, suffered from intrinsic defects at SiO_2/Si(100) interfaces.[3] These intrinsic defects are increasingly important since atomic-layer Si oxide is indispensable even under high-k dielectrics. Unsaturated dangling bonds (DB), referred to as P_b defects, are constantly generated at the interfaces between SiO_2 and the Si substrate from the early stage of oxidation.[4] This behavior is well detected by ESR techniques.[5] For P_b centers at the SiO_2/Si(100) interface, P_{b0} and P_{b1} have been clearly distinguished and are observed simultaneously.[6] The P_{b0} center has a microscopic character with an isolated sp^3 DB pointing into the $\langle 111\rangle$ direction, while the P_{b1} center has an isolated DB pointing into $\langle 211\rangle$ direction. Both types of P_b center have been identified as a $^{\cdot}Si\equiv Si_3$ with no O atom in the Si back bonds as a result of good agreement between experimentally observed and theoretically proposed hyperfine interactions.[7,8] Through extensive theoretical studies on the early stage of Si(100) oxidation with over 100 oxidized configurations, we have clearly explained the P_{b0} center generation mechanism and have proposed overall structures including trimers.[9] On the other hand, although the model structure of the P_{b1} center and its hyperfine interactions were characterized and agree well with experimental results,[7] why such a strange structure of P_{b1} centers can be generated and why it stably exists in contrast to a plausible structure of P_{b0} centers are not well understood. It is also not clear why P_b centers have no O atom in the back bonds and whether or not both P_{b0} and P_{b1} centers exist stably at the same SiO_2/Si(100) interface layer.

The aims of the present paper are to propose the atomic processes of P_{b1} center generation and to elucidate the electronic structures of P_{b1} centers in Si(100) oxidation through first-principles theoretical calculations. To create a more favorable situation for analysis, we used an oxidized Si(100) surface, which is realized mostly by adding O atoms between Si DBs on topmost surfaces and between Si bond-centers on a clean Si(100) surface.[9] Our calculations are based on density functional theory (DFT) and generalized gradient approximation (GGA) to describe oxygen properties properly.[10] The calculations are performed using ultrasoft pseudopotentials[11] for O and H atoms with 1 k to 4 k points for Brillouin zone samplings. We found that the cutoff energies of 25 Ry for the wave functions and 144 Ry for the augmented electron densities are sufficient for converging energies. All the calculations were performed with a repeated slab modified from a (2×6) surface unit cell, consisting of 14 layers of Si atoms and a vacuum spacing with the same thickness. Inversion symmetry with respect to the slab center located at an Si bond center is used to increase the computational efficiency. The hyperfine axis was evaluated for $Si_{13}(O_2)H_9$ structures with all-electron calculations.[12]

Before going into the calculations, we will look into SiO_2/Si(100) interface structures[13,14] involving P_b centers. As oxidation of Si(100) progresses from the topmost surface with O_2 dissociation,[15] volume expansion of SiO_2 occurs, generating strong internal stresses accordingly. These stresses, in some cases, make the second-neighbor atoms come closer. First, we consider the stage where substantial Si layers are oxidized, as shown in the (110) cross-sectional view of Fig. 1(a). When both Si bonds of Si(3)-Si(1) and of Si(2)-Si(5) are oxidized as Si(3)-O-Si(1)-Si(4)-Si(2)-O-Si(5), Si(1) and Si(2) inevitably come closer to each other.[16] Indeed, as shown in Fig. 1(b), another O atom was theoretically proven to form a bridge bond between Si(1) and Si(2) as Si(3)-O-Si(1)-O-Si(2)-O-Si(5) rather than falling into a tight Si bond center.[9] We hereafter denote the O atom in the bridge bond as BBO.

Figure 2 illustrates typical BBO formation processes in the $(1\bar{1}0)$ cross-sectional view with 90° rotation about the

 ©2006 The American Physical Society

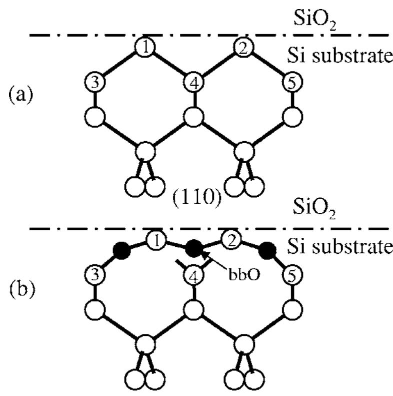

FIG. 1. $SiO_2/Si(100)$ interfaces in the (110) cross section (a) with an atomically flat normal structure, (b) with bridge-bond oxidation of structure (a). Dark circles represent O atoms, and bright circles represent Si atoms.

interface normal. Figure 2(a) corresponds to the oxidation advancing stage where the $SiO_2/Si(100)$ interface is atomically flat.[1] Here, we present a scenario to account for those experimentally and theoretically proven aspects of P_b centers, where P_{b0} and P_{b1} are generated corresponding to locations of BBO formation. When the BBOs shown in Fig. 1(b) are formed alternately at every second site in the next-layer oxidation stage Si(1), Si(3), and Si(5) shown in Fig. 2(b) may be emitted as interstitial Si atoms. Then, Si trimers of Si(2)-Si(7)-Si(8) and of S(4)-Si(9)-Si(10) are formed to reduce generated DBs below the oxidized sites. Both sides of one trimer row generate P_{b0} centers.[9] On the other hand, when O atoms form bridge bonds alternately for the most part, but occasionally at two adjacent sites, as shown in Fig. 2(c), the Si(2), Si(3), Si(5), and Si(6′) may be emitted as an interstitial Si atom. Then, an Si dimer is formed by shifting Si(8) left toward Si(7), and Si trimers of Si(4)-Si(9)-Si(10)

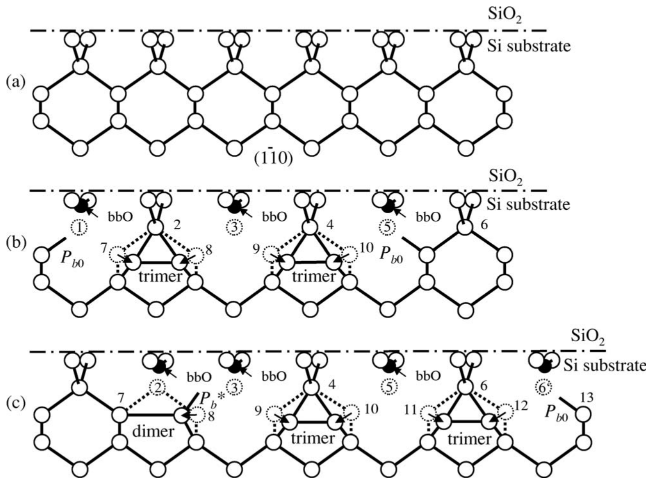

FIG. 2. $SiO_2/Si(100)$ interfaces in the $(1\bar{1}0)$ cross section (a) with an atomically flat normal structure, (b) with P_{b0} defects generated at both sides by alternate bridge-bond oxidation of structure (a), and (c) with P_b^* and P_{b0} defects generated on both sides by almost alternate but two-adjacent bridge-bond oxidation of structure (a). Dark circles represent O atoms, and bright circles represent Si atoms.

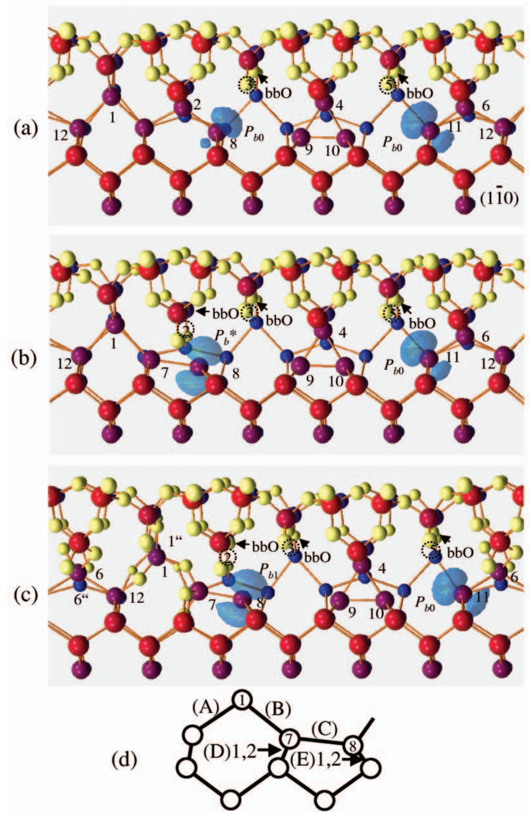

FIG. 3. (Color) $SiO_2/Si(100)$ interfaces in the $(1\bar{1}0)$ cross section for the early stage oxidation (a) where P_{b0} defects are generated by alternate bridge-bond oxidation, (b) where P_b^* and P_{b0} defects are generated by almost alternate but two-adjacent bridge-bond oxidation for the structure (a), and (c) where lateral oxidation continues for structure (b). White balls represent O atoms. Red and blue balls represent Si atoms. Blue isosurfaces represent DBs at P_{b1} and P_{b0} centers. (d) Possible oxidation sites (A), (B), (C), (D), and (E) around P_b^* for structure (b).

and of Si(6)-Si(11)-Si(12) are formed, reducing excess energy associated with DBs below the oxidized sites. The right side generates a P_{b0} center, but the left side forming a dimer bond generates a new P_b center. This is the principal mechanism of new P_b generation at the $SiO_2/Si(100)$ interface, being clearly distinguished from P_{b0} center generation. The structure of this P_b center corresponds well with the Dimer model previously proposed for a P_{b1} center,[8,17] but this model failed to account for the experimentally observed hyperfine axis orientation. The asymmetrically oxidized dimer (AOD) model recently proposed for a P_{b1} center,[7] on the other hand, satisfies the overall hyperfine parameters well. The orientation of the DB axis for the AOD model is much closer to the experimental observations compared with the Dimer model, because site (D) denoted in Fig. 3(d) is oxidized, while oxidation does not occur at the P_{b1} back bonds. This idea leads us to ask why site (D) can be oxidized without oxidation at the P_{b1} back bonds.

In the early stages of oxidation on Si(100) surfaces, the oxidized structure reflects surface dimer rows running along the $[1\bar{1}0]$ axis. Figure 3(a) shows a calculated Si(100) struc-

ture oxidized one monolayer. We denote here that one monolayer oxidation includes back-bond oxidation of the topmost Si atoms. O atoms are placed in Si-Si bonds successively from the topmost surface to deeper regions, and the oxidized structure is relaxed accordingly to realize the most stable structure.[9] The surface dimer-row structures promote alternate BBO formation, as compared with the oxidation at atomically flat $SiO_2/Si(100)$ interfaces as explained in Fig. 2(b). At the back-bond oxidation stage as shown in Fig. 3(a), bridge-bond oxidation occurs alternately at every second site. Only one trimer of Si(4)-Si(9)-Si(10) was formed because of a relatively small (2×6) unit cell after emission of Si(3) and Si(5) below the oxidized sites, as found in our previous work.[9] P_{b0} centers are generated first on both sides in the fourth layer after 1 monolayer oxidation. As O atoms form bridge bonds alternately for the most part, but occasionally at two adjacent sites as shown in Fig. 3(b), Si(2), which is located deeper than Si(3) and Si(5), is emitted as an interstitial Si atom. Then, a new P_b center is formed on the left side with the same mechanism as described for Fig. 2(c). Here, we named it as P_b^*. The new P_b^* is thus generated first after P_{b0} center generation even in the initial stage of oxidation, corresponding well with observations by ESR measurement.[18] The energy gain by forming one dimer and one trimer is a negative value of −0.32 eV. This is because the dimer and trimer formation gains energy, but more energy is lost from breaking the weak bonds of Si(8)-Si(9) and Si(10)-Si(11). The energy gain, however, turned out be a positive value, as more than two trimers are lined up along the [110] axis. It increases to a maximum value of 0.49 eV/trimer.[9] The distance between P_{b0} and P_b^* centers will be, therefore, much greater in reality. The orientation of the DB axis in this P_b^* center from the interface normal is, however, 19°, being much smaller than the experimentally observed hyperfine axis which is 32.3° from the interface normal.[6] When we compare the energy of P_b^* and P_{b0} centers with the same number of Si and O atoms, the energy cost for P_b^* generation is 1.8 eV higher than that for P_{b0} generation. This is presumably due to internal strains generated by atomically nonuniform $SiO_2/Si(100)$ interfaces. This structure is potentially generated but with a low probability. The other sites may be oxidized before P_b^* generation.

Hence, we explored the other possible oxidation sites (A), (B), (C), (D), and (E) around the P_b^* center, as shown in Fig. 3(d). Bonds above Si(1) and its inside Si(1″) atoms were oxidized beforehand, as shown in Fig. 3(c). If oxidation at (D) is favored over oxidation at (E), the orientation of the DB axis in the P_b^* center will come closer to the experimentally observed hyperfine axis orientation as of the AOD model.[7] The energy gains from oxidation at the (A), (B), (C), (D), and (E) sites were calculated to be 7.49, 7.51, 7.09, 5.81, and 6.88 eV, respectively. The oxidation at (C) will lead to elongation of the bond between Si(7) and Si(8), shifting Si(8) toward Si(9). This shift forms a weak bond between Si(8) and Si(9), resulting in P_b^* destruction. Therefore, oxidation at (C) can be neglected in this argument. For (D) and (E), the energy gains were averaged over (D)1 and (D)2, and over (E)1 and (E)2, respectively. The energy gain from oxidation at (D) for the (A) and (B) preoxidized structure is increased merely up to 6.22 eV, still lower than the energy gain from oxidation at (E). Preferential oxidation at (D) does not occur in this situation. The energy gain from oxidation at (E) does not change even if O atoms are placed from the topmost surface in a layer-by-layer manner.

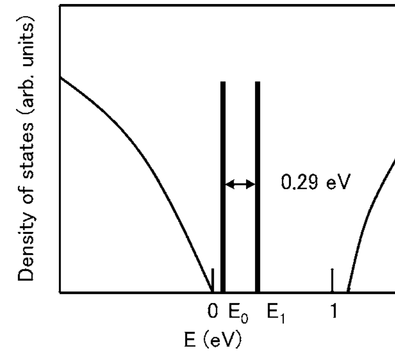

FIG. 4. Schematic densities of states in the vicinity of the Si band gap. Gap states corresponding to P_{b0} and P_{b1} centers are denoted by E_0 and E_1.

Then, we continued the lateral oxidation in a layer-by-layer manner, forming an energetically stable structure.[9] The back bonds of Si(1) and its inside Si(1″) atoms were fully oxidized. The bonds above Si(6) and its inside Si(6″) atoms were also oxidized, as shown in Fig. 3(c). Then, site (D) in Fig. 3(d) is oxidized in this structure, as displayed in Fig. 3(c). The oxidation energy gain at (D) is increased up to 7.54 eV [larger than at (E)] because of local strain energy release at the back bonds of the Si(1″) atom at the inside location of the Si(1) atom. This structure exists stably, being geometrically close to the possible structure AOD for P_{b1}.[7] The orientation of the DB axis in this P_{b1} center from the interface normal is 26° while the orientation of the possible structure AOD is 33°. The discrepancy from the experimentally observed value of 32.3° is primarily due to large stress in the vicinity of P_{b1} in a small (2×6) unit cell. Si atoms below the P_{b1} center are constrained along the $[1\bar{1}0]$ direction because of the small unit cell along the [110] direction. In addition, we cannot neglect the possible existence of P_b^* with a lower orientation axis as shown in Fig. 3(b) at $SiO_2/Si(100)$ interfaces. In this way, we prove that both P_{b0} and P_{b1} can simultaneously exist at the same $SiO_2/Si(100)$ interface. As oxidation progresses further, the oxide thickness deviation will be reduced, and the difference in energy cost between the alternate BBO generation and the successive BB0 generation will be reduced. Then, the generation probability of the P_{b1} center will be increased.

Now, we examine the electronic structures of P_b centers. The densities of states in the vicinity of the Si band gap are schematically shown in Fig. 4. Gap states corresponding to P_{b0} at Si(8) and P_{b1} at Si(11) are denoted by E_0 and E_1. Since the structure still has dispersion along the $[1\bar{1}0]$ axis because of the relatively small (2×6) unit cell, the calculations were sampled over 4 k points along the $[1\bar{1}0]$ axis. To avoid the mutual hybridization, either Si(11) or Si(8) was terminated by an H atom for P_{b0} and P_{b1} center evaluation, respectively. Then, E_0 and E_1 were estimated to be

0.07 ± 0.02 and 0.36 ± 0.10 eV from the top of the valence band, and both levels lie lower than the midgap of the Si band gap. Those electronic structures correspond well to the experimentally observed $+/0$ levels.[19]

The highest occupied states (less than 0.2 eV below the Fermi level) and the lowest unoccupied states (less than 0.2 eV above the Fermi level) are displayed by blue isosurfaces in Figs. 3(b) and 3(c). Si(8) and Si(11) maintain a weak interaction because of the relatively short distance of 1.2 nm. Corresponding to the energy levels of P_{b0} and P_{b1}, the dominantly occupied P_{b0} denoted by the blue isosurface on the right side looks similar to an sp^3 orbital, while the unoccupied P_{b1} denoted by the blue isosurface on the left side looks closer to a higher p orbital rather than a lower sp^3 orbital. In contrast, the highest occupied states (less than 0.2 eV below the Fermi level) denoted with blue isosurfaces in Fig. 3(a) are divided almost evenly between the two P_{b0} centers.

In summary, we presented generation mechanisms for P_b centers, especially for the P_{b1} center, which agree well with the atomic and electronic structures of P_b centers reported by theoretical and experimental studies. The P_{b0} center appears first and the P_{b1} center appears later, agreeing with experimental observation. We proved that the P_{b1} center is generated without any O atom in the back bonds, and that both the P_{b0} and P_{b1} centers exist simultaneously at the same Si/SiO_2 interface. The energy level of the P_{b1} center is slightly higher than that of the P_{b0} center, corresponding well with the experimental observation.

We would like to thank S. Yamasaki, W. Futako, and T. Yasuda for valuable discussions and suggestions.

[1] H. Watanabe, K. Kato, T. Uda, K. Fujita, M. Ichikawa, T. Kawamura, and K. Terakura, Phys. Rev. Lett. **80**, 345 (1998).

[2] T. Yasuda, S. Yamasaki, M. Nishizawa, N. Miyata, A. Shklyaev, M. Ichikawa, T. Matsudo, and T. Ohta, Phys. Rev. Lett. **87**, 037403 (2001); T. Yasuda, N. Kumagai, M. Nishizawa, S. Yamasaki, H. Oheda, and K. Yamabe, Phys. Rev. B **67**, 195338 (2003).

[3] A. Stesmans and V. V. Afanas'ev, J. Appl. Phys. **83**, 2449 (1998).

[4] W. Futako, N. Mizuochi, and S. Yamasaki, Phys. Rev. Lett. **92**, 105505 (2004).

[5] T. Umeda, M. Nishizawa, T. Yasuda, J. Isoya, S. Yamasaki, and K. Tanaka, Phys. Rev. Lett. **86**, 1054 (2001).

[6] A. Stesmans and V. V. Afanas'ev, Phys. Rev. B **57**, 10030 (1998).

[7] A. Stirling, A. Pasquarello, J.-C. Charlier, and R. Car, Phys. Rev. Lett. **85**, 2773 (2000).

[8] A. Stesmans, B. Nouwen, and V. V. Afanas'ev, Phys. Rev. B **58**, 15801 (1998).

[9] T. Yamasaki, K. Kato, and T. Uda, Phys. Rev. Lett. **91**, 146102 (2003).

[10] J. P. Perdew, in *Proceedings of Electronic Structure of Solids '91*, edited by P. Ziesche and H. Eschrig (Academic Verlag, Berlin, 1991), p. 11.

[11] D. Vanderbilt, Phys. Rev. B **41**, 7892 (1990).

[12] M. J. Frisch *et al.*, *Gaussian 03*, Revision B.04 (Gaussian, Inc., Pittsburgh PA, 2003).

[13] A. Pasquarello, M. S. Hybersten, and R. Car, Nature (London) **396**, 58 (1998).

[14] T. Yamasaki, C. Kaneta, T. Uchiyama, T. Uda, and K. Terakura, Phys. Rev. B **63**, 115314 (2001).

[15] K. Kato, T. Uda, and K. Terakura, Phys. Rev. Lett. **80**, 2000 (1998); K. Kato and T. Uda, Phys. Rev. B **62**, 15978 (2000).

[16] H. Kageshima and K. Shiraishi, Phys. Rev. Lett. **81**, 5936 (1998).

[17] A. H. Edwards, in *The Phisics and Chemistry of* SiO_2 *and the* SiO_2 *Interface*, edited by C. R. Helms and B. E. Deal (Plenum, New York, 1988), p. 271.

[18] S. Yamasaki and W. Futako (private communication).

[19] J. P. Campbell and P. M. Lenahan, Appl. Phys. Lett. **80**, 1945 (2002).